Finite Volume Structure-Preserving Discretization of 1D Distributed-Parameter Port-Hamiltonian Systems

Paul Kotyczka

Finite Volume Structure-Preserving Discretization of 1D Distributed-Parameter Port-Hamiltonian Systems

Paul Kotyczka *

* *Laboratoire d'Automatique et de Génie des Procédés (LAGEP), Université Claude Bernard Lyon 1, 69622 Villeurbanne, France (e-mail: kotyczka@tum.de).*

Abstract: A family of finite-dimensional approximate models is proposed which preserves the port-Hamiltonian structure of a class of open systems of conservation laws. The approach is based on conservative generalized leapfrog schemes with given consistency orders in terms of their stencil. The finite volume perspective fits naturally to the formulation of the conservation laws on staggered grids. Some observations on current structure-preserving discretization methods are discussed and related to the proposed approach. A frequently used benchmark example highlights some of the method's properties and differences to existing structure-preserving schemes.

Keywords: Port-Hamiltonian systems, systems of conservation laws, distributed-parameter systems, semi-discretiziation, finite volume methods.

1. INTRODUCTION

The port-Hamiltonian (PH) representation of open systems of conservation laws [van der Schaft and Maschke 2002] captures their physical (interconnection) structure and in particular includes the expression of boundary port variables to describe the energy exchange with the environment. The latter is a prerequisite for boundary control, where the PH structure again is favorable in terms of well-posedness and the application of energy-based methods, see e. g. Ramirez et al. [2014]. A discretization of the underlying partial differential equations is necessary for simulation and, even more if nonlinear systems are considered, for manageable controller design. Different approaches for spatial semi-discretization which preserve the PH structure and in particular the power balance have been reported.

The core idea of structure-preserving semi-discretization methods for PH systems is to account for the different geometric nature of the power variables (efforts and flows) in the numerical approximation of their spatial distributions. Existing works are based on a (mixed) finite element (FE) perspective, using simple approximation forms on every segment [Golo et al. 2004] or higher order polynomials to approximate the distributed power variables at collocation points [Moulla et al. 2012]. A partial permutation of the canonical roles of energy and co-energy variables allows formulating an alternative structure-preserving discretization scheme [Farle et al. 2013].

For systems of conservation laws, there exists a multitude of finite volume (FV) / finite difference (FD) discretization schemes in space (semi-discretization) or in space and time (full-discretization) with different characteristic properties to simulate various systems and application cases. Find an overview of FD and FV methods for example in LeVeque [1992], LeVeque [2002], Eymard et al. [2000]. Among these methods, *conservative* schemes such as the *generalized leapfrog* methods [Iserles 1986] do not introduce numerical dissipation.

The purpose of this paper is to show that the semi-discrete versions of generalized leapfrog schemes are a very natural basis to formulate structure-preserving discretization methods for open PH systems of conservation laws. Thereby, naturally, special attention is paid to the definition of boundary port variables.

The paper is organized as follows. In Section 2, preliminaries on FV methods on staggered grids, semi-discrete leapfrog schemes and the PH representation of systems of two conservation laws in 1D are presented. Besides the distributed-parameter point of view, a discrete system representation on staggered grids, which serves as basis for the FV schemes in Section 4, is introduced. In Section 3, some observations on structure-preserving discretization of PH systems with current methods are summarized. Section 4 presents as a main result the class of FV semi-discretization methods for open PH systems. In Section 5, the illustrative example from Golo et al. [2004] is used for a first discussion and comparison of the presented approach. Section 6 concludes the paper with open questions and an outlook to further work.

⋆ The author is on leave from Technical University of Munich at LAGEP with an Individual Fellowship of the European Commission's Marie Skłodowska-Curie Actions, Call H2020-MSCA-IF-2014_ST, Proposal No. 655204, EasyEBC – Easy-to-Implement Energy-Based Control Design for Systems of Conservation Laws.

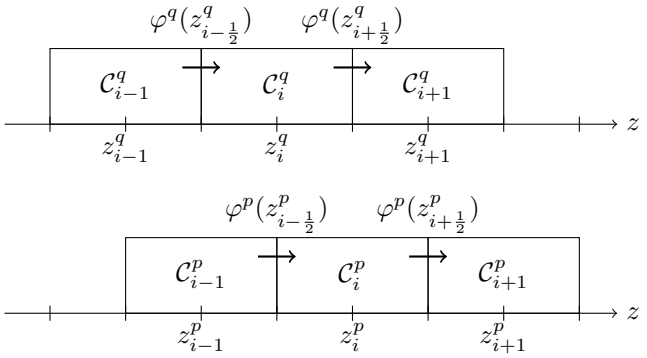

Fig. 1. Cells on both grids; fluxes at the cell boundaries.

2. PRELIMINARIES

2.1 Systems of two conservation laws

The dynamics of a (time-invariant) system of two conservation laws on a one-dimensional spatial domain can be represented in integral form by the equations [1]

$$\frac{d}{dt}\int_{\mathcal{C}^q_i} q(z,t)\,dz = \varphi^q(q,p,z^q_{i-1/2},t) - \varphi^q(q,p,z^q_{i+1/2},t) \quad (1)$$

$$\frac{d}{dt}\int_{\mathcal{C}^p_i} p(z,t)\,dz = \varphi^p(q,p,z^p_{i-1/2},t) - \varphi^p(q,p,z^p_{i+1/2},t). \quad (2)$$

$q(z,t)$, $p(z,t)$ are the conserved quantities, $\mathcal{Z} = [z_L, z_R]$ the spatial domain, $\mathcal{C}^q_i, \mathcal{C}^p_i$ are cells on the grid for the q and the p variable, respectively. φ^q, φ^p denote flux functions which are evaluated at the cell boundaries. z^q_i, z^p_i are the spatial coordinates of the cell centers. As depicted in Fig. 1, we consider *shifted* or *staggered* grids. This point of view, which is instrumental for achieving a certain consistency order with *generalized leapfrog* numerical schemes [Iserles 1986] can be found already in Yee et al. [1966] for the numerical simulation of Maxwell's equations. In differential form, (1), (2) correspond to

$$\frac{d}{dt}\begin{bmatrix} q(z,t) \\ p(z,t) \end{bmatrix} = -\frac{\partial}{\partial z}\begin{bmatrix} \varphi^q(q,p,z,t) \\ \varphi^p(q,p,z,t) \end{bmatrix} \quad (3)$$

with initial conditions $q(z,0)$, $p(z,0)$ and the corresponding boundary conditions on φ^q, φ^p at $z = z_L$, $z = z_R$.

Example. For the linear wave equation in first order representation we have $\varphi^q = p$, $\varphi^p = q$, and hence

$$\frac{d}{dt}\int_{\mathcal{C}^q_i} q(z,t)\,dz = p(z^q_{i-1/2},t) - p(z^q_{i+1/2},t) \quad (4)$$

$$\frac{d}{dt}\int_{\mathcal{C}^p_i} p(z,t)\,dz = q(z^p_{i-1/2},t) - q(z^p_{i+1/2},t). \quad (5)$$

2.2 Finite volume numerical schemes

A finite volume numerical scheme for this class of systems has the general structure [2]

$$\frac{d}{dt}Q_i = \phi^q_{i-1/2} - \phi^q_{i+1/2} \quad (6)$$

$$\frac{d}{dt}P_i = \phi^p_{i-1/2} - \phi^p_{i+1/2}. \quad (7)$$

[1] $\varphi^q(q,p,z^q_{i-1/2},t)$ abbreviates $\varphi^q(q(z^q_{i-1/2},t), p(z^q_{i-1/2},t))$, etc.

[2] The time dependency is skipped for brevity.

Table 1. Coefficients for semi-discrete generalized leapfrog schemes with order $2r$

r	a_1	a_2	a_3
1	1		
2	$\frac{9}{8}$	$-\frac{1}{24}$	
3	$\frac{75}{64}$	$-\frac{25}{384}$	$\frac{3}{640}$

We denote

$$Q_i \approx \int_{\mathcal{C}^q_i} q(z)\,dz, \qquad P_i \approx \int_{\mathcal{C}^p_i} p(z)\,dz \quad (8)$$

the numerical approximations of the integral conserved quantities on each cell and

$$\phi^q_{i\pm1/2} \approx \varphi^q(q,p,z^q_{i\pm1/2}), \quad \phi^p_{i\pm1/2} \approx \varphi^p(q,p,z^p_{i\pm1/2}) \quad (9)$$

the approximations of the boundary fluxes. These are computed from *numerical flux functions*, incorporating a finite number of approximate cell states Q_i, P_i, according to the *stencil* of the method. The simplest conservative finite volume method is the *leapfrog scheme* see e. g. Rezzolla [2011].

Example. The semi-discrete version (only in space) of the leapfrog scheme for the linear wave equation is

$$\begin{aligned} \dot{Q}_i &= \phi^q_{i-1/2} - \phi^q_{i+1/2} = P_{i-1} - P_i, \\ \dot{P}_i &= \phi^p_{i-1/2} - \phi^p_{i+1/2} = Q_i - Q_{i+1}. \end{aligned} \quad (10)$$

This numerical scheme has a consistency order of 2 in space and also in time, if an appropriate centered time integration step is considered [Iserles 1986], [Rezzolla 2011].

Higher consistency order of $2r$ with $r > 1$ can be obtained by *generalized leapfrog schemes* as presented in Iserles [1986] for the advection equation. $2r$ cells are taken into account to compute the net numerical fluxes into each cell.

Example. The generalized leapfrog scheme, adapted to the linear wave equation, reads

$$\begin{aligned} \dot{Q}_i &= \sum_{k=1}^{r} a_k (P_{i-k} - P_{i-1+k}) \\ \dot{P}_i &= \sum_{k=1}^{r} a_k (Q_{i+1-k} - Q_{i+k}). \end{aligned} \quad (11)$$

By computing the coefficients $1 \le k \le r$ according to [3]

$$a_k = (-1)^{r-k} \frac{(\mu - r + \frac{1}{2})_{2r}}{(\mu - r + \frac{1}{2})(\mu + r - \frac{1}{2})(r-k)!(r-1+k)!}, \quad (12)$$

a consistency order of $2r$ in space is achieved. $\mu = \Delta t/\Delta z$ is the Courant number. With a centered scheme for time discretization, the correct μ has to be replaced. For the semi-discrete case with $\mu = 0$, the coefficients as in Table 5 of Fornberg and Ghrist [1999] are obtained.

2.3 Port-Hamiltonian systems of two conservation laws

In port-Hamiltonian form, the boundary fluxes are identified with point-wise evaluations of the *effort variables* on the dual grid. The latter are the variational derivatives

$$e^q(q,p,z) = \delta_q H(q,p), \quad e^p(q,p,z) = \delta_p H(q,p) \quad (13)$$

[3] This is the semi-discrete version of the corresponding formula in Lemma 2 of Iserles [1986].

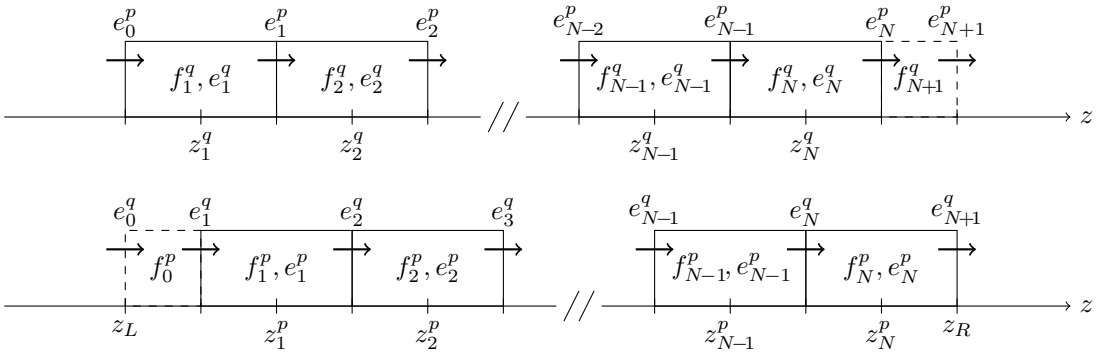

Fig. 2. Discrete representation of a system of two conservation laws with staggered control volumes (intervals). The boundary fluxes $e^p_0 = e^p(z_L)$ and $e^q_{N+1} = e^q(z_R)$ are considered inputs, $e^q_0 = e^q(z_L)$ and $-e^p_{N+1} = -e^p(z_R)$ collocated outputs. For the numerical schemes, the dashed control volumes are neglected, and $e^q_0 \approx e^q_1$, $e^p_N \approx e^p_{N+1}$ is assumed.

of the total stored energy or Hamiltonian

$$H(q,p) = \int_0^L \mathcal{H}(q(z), p(z), z)\, dz. \tag{14}$$

with $\mathcal{H}$ the Hamiltonian density. The PH dynamics in integral form is then given by [4],

$$\frac{d}{dt}\int_{\mathcal{C}^q_i} q(z,t)\, dz = e^p(q,p,z^p_{i-1},t) - e^p(q,p,z^p_i,t) \tag{15}$$

$$\frac{d}{dt}\int_{\mathcal{C}^p_i} p(z,t)\, dz = e^q(q,p,z^q_i,t) - e^q(q,p,z^q_{i+1},t), \tag{16}$$

or, in differential form,

$$\frac{d}{dt}\begin{bmatrix} q(z,t) \\ p(z,t)\end{bmatrix} = \begin{bmatrix} 0 & -1 \\ -1 & 0\end{bmatrix}\frac{\partial}{\partial z}\begin{bmatrix} e^q(z,t) \\ e^p(z,t)\end{bmatrix} \tag{17}$$

with appropriate initial and boundary conditions.

Example. The linear wave equation from the above examples is recovered when $\mathcal{H}(q,p) = \frac{q^2}{2} + \frac{p^2}{2}$.

A salient property of the PH representation is that, from the structure of the equations, using integration by parts (or Stokes theorem in more than one spatial dimension), the following power balance equation [5] is obtained:

$$\dot{H} = \int_{z_L}^{z_R} e^q(z)\dot{q}(z) + e^p(z)\dot{p}(z)\, dz = -\left[e^q(z)e^p(z)\right]_{z_L}^{z_R}. \tag{18}$$

Stokes-Dirac structure. In a more formal way, see van der Schaft and Maschke [2002] for details, the power balance equation can be expressed as the *non degenerate bilinear form*, associated to the *Stokes-Dirac structure* on the space $\mathcal{F}\times\mathcal{E}$ defined by

$$\mathcal{F} = \Omega^1(\mathcal{Z})\times\Omega^1(\mathcal{Z})\times\Omega^0(\partial\mathcal{Z}) \ni (f^q, f^p, \boldsymbol{f}^b) \tag{19}$$

$$\mathcal{E} = \Omega^0(\mathcal{Z})\times\Omega^0(\mathcal{Z})\times\Omega^0(\partial\mathcal{Z}) \ni (e^q, e^p, \boldsymbol{e}^b) \tag{20}$$

with the one-forms (*flow* variables in $\Omega^1(\mathcal{Z})$)

$$f^q = \dot{q}(z)\, dz, \qquad f^p = \dot{p}(z)\, dz, \tag{21}$$

the zero-forms (*effort* variables in $\Omega^0(\mathcal{Z})$) as defined above and the boundary variables (in $\Omega^0(\partial\mathcal{Z})$), defined e. g. as

$$\boldsymbol{e}^b = \begin{bmatrix} e^p(z_L) \\ e^q(z_R)\end{bmatrix}, \quad -\boldsymbol{f}^b = \begin{bmatrix} e^q(z_L) \\ -e^p(z_R)\end{bmatrix}. \tag{22}$$

[4] Note that we have replaced $z^q_{i-1/2} = z^p_{i-1}$, $z^p_{i-1/2} = z^q_i$, etc.

[5] Using the definition of the variational derivative and taking $\dot{q}$ and $\dot{p}$ as variations

The above-mentioned bilinear form to express the balance equation is then

$$\langle (e^q, e^p, \boldsymbol{e}^b) | (f^q, f^p, \boldsymbol{f}^b)\rangle = \int_Z [e^q \wedge f^q + e^p \wedge f^p] + \langle \boldsymbol{e}^b, \boldsymbol{f}^b\rangle \tag{23}$$

with $\wedge$ the exterior product between two differential forms, $\langle\cdot,\cdot\rangle$ the standard inner product on Euclidean space. Power-preservation is expressed by

$$\langle (e^q, e^p, \boldsymbol{e}^b) | (f^q, f^p, \boldsymbol{f}^b)\rangle = 0. \tag{24}$$

Discrete representation. As a whole, the system of two conservation laws can be represented in integral form by

$$\frac{d}{dt}\int_{z_L}^{z_R} q(z)\, dz = e^p(z_L) - e^p(z_R) \tag{25}$$

$$\frac{d}{dt}\int_{z_L}^{z_R} p(z)\, dz = e^q(z_L) - e^q(z_R), \tag{26}$$

which gives *no information about the spatial distribution* of the energy variables (states) $q(z)$ and $p(z)$. Dividing the spatial domain into the intervals

$$\mathcal{C}^q_i = \begin{cases} [z_L, z^p_1] & i = 1, \\ (z^p_{i-1}, z^p_i] & i = 2,\ldots,N, \end{cases} \tag{27}$$

$$\mathcal{C}^p_i = \begin{cases} [z^q_i, z^q_{i+1}) & i = 1,\ldots,N-1, \\ [z^q_N, z_R] & i = N, \end{cases} \tag{28}$$

the conservation laws can be rewritten, $i = 1,\ldots,N$,

$$\frac{d}{dt}\int_{\mathcal{C}^q_i} q(z)\, dz = e^p(z^p_{i-1}) - e^p(z^p_i), \tag{29}$$

$$\frac{d}{dt}\int_{\mathcal{C}^p_i} p(z)\, dz = e^q(z^q_i) - e^p(z^q_{i+1}), \tag{30}$$

with $z^p_0 = z_L$, $z^q_{N+1} = z_R$. Define for $i = 1,\ldots,N$

$$f^q_i := \frac{d}{dt}\int_{\mathcal{C}^q_i} q(z)\, dz, \qquad f^p_i := \frac{d}{dt}\int_{\mathcal{C}^p_i} p(z)\, dz, \tag{31}$$

as flow variables and the point-wise values of the distributed efforts

$$e^q_i := e^q(z^q_i), \qquad e^p_i := e^p(z^p_i) \tag{32}$$

as efforts and collect them in the vectors

$$\boldsymbol{f}^q = \begin{bmatrix} f^q_1 \\ \vdots \\ f^q_N\end{bmatrix}, \ \boldsymbol{f}^p = \begin{bmatrix} f^p_1 \\ \vdots \\ f^p_N\end{bmatrix}, \ \boldsymbol{e}^q = \begin{bmatrix} e^q_1 \\ \vdots \\ e^q_N\end{bmatrix}, \ \boldsymbol{e}^p = \begin{bmatrix} e^p_1 \\ \vdots \\ e^p_N\end{bmatrix}. \tag{33}$$

With the boundary efforts $e_0^p := e^p(z_L)$ and $e_{N+1}^q := e^q(z_R)$, a discrete version of (29), (30) is

$$\boldsymbol{f}^q = \underbrace{\begin{bmatrix} -1 & & & \\ 1 & -1 & & \\ & \ddots & \ddots & \\ & & 1 & -1 \end{bmatrix}}_{\boldsymbol{D}} \boldsymbol{e}^p + \underbrace{\begin{bmatrix} 1 \\ 0 \\ \vdots \\ 0 \end{bmatrix}}_{\boldsymbol{g}_q} e_0^p \tag{34}$$

$$\boldsymbol{f}^p = \underbrace{\begin{bmatrix} 1 & -1 & & \\ & \ddots & \ddots & \\ & & 1 & -1 \\ & & & 1 \end{bmatrix}}_{-\boldsymbol{D}^T} \boldsymbol{e}^q + \underbrace{\begin{bmatrix} 0 \\ \vdots \\ 0 \\ -1 \end{bmatrix}}_{\boldsymbol{g}_p} e_{N+1}^q. \tag{35}$$

Note however that in this discrete formulation of the conservation laws, the flows and the efforts are both defined in terms of the distributed states $q(z)$, $p(z)$, whose evolution obey the corresponding PDE (17).

For the dashed boundary cells in Fig. 2, which have not been considered so far, we have

$$f_0^p = e_0^q - e_1^q, \quad f_{N+1}^q = e_N^p - e_{N+1}^p. \tag{36}$$

Expressing the (lumped) power balance over all $2N$ interior (solid) cells, we get

$$\begin{aligned} &\langle \boldsymbol{e}^q, \boldsymbol{f}^q \rangle + \langle \boldsymbol{e}^p, \boldsymbol{f}^p \rangle \\ &\quad = (\boldsymbol{e}^q)^T (\boldsymbol{D}\boldsymbol{e}^p + \boldsymbol{g}_q e_0^p) + (\boldsymbol{e}^p)^T (-\boldsymbol{D}^T \boldsymbol{e}^q + \boldsymbol{g}_p e_{N+1}^q) \\ &\quad = \underbrace{(\boldsymbol{e}^q)^T \boldsymbol{g}_q}_{e_1^q = e_0^q - f_0^p} e_0^p + \underbrace{(\boldsymbol{e}^p)^T \boldsymbol{g}_p}_{-e_N^p = -e_{N+1}^p - f_{N+1}^q} e_{N+1}^q. \end{aligned}$$

The definition of boundary port variables, i. e. in- and output variables of the boundary control systems,

$$\boldsymbol{e}^b = \begin{bmatrix} e_0^p \\ e_{N+1}^q \end{bmatrix}, \quad -\boldsymbol{f}^b = \begin{bmatrix} e_0^q(-f_0^p) \\ -e_{N+1}^p(-f_{N+1}^q) \end{bmatrix}, \tag{37}$$

is in accordance with (22), except for the terms in brackets. The slight non-collocation is due to the staggered grids and vanishes with $\Delta z \to 0$. Hence, the discrete analogue of Eq. (23) is

$$\langle \boldsymbol{e}^q, \boldsymbol{f}^q \rangle + \langle \boldsymbol{e}^p, \boldsymbol{f}^p \rangle + \langle \boldsymbol{e}^b, \boldsymbol{f}^b \rangle = 0. \tag{38}$$

Remark 1. Note that the roles of in- and outputs can be permuted by shifting the grids in opposite direction. In this paper only the situation depicted in Fig. 2 is considered.

3. OBSERVATIONS ON STRUCTURE-PRESERVING DISCRETIZATION OF PH SYSTEMS

Structure-preserving discretization schemes aim at a finite-dimensional approximation of the infinite-dimensional PH dynamics which is in PH form and can be understood as the explicit representation of an approximation Dirac structure. Current methods [Golo et al. 2004, Farle et al. 2013] are based on a mixed finite element perspective, exploit a direct formulation of discrete conservation laws on dual meshes [Seslija et al. 2014] or use a pseudo-spectral collocation approach [Moulla et al. 2012]. In this section, some observations on current structure-preserving methods, which have a direct relation to the present work, shall be summarized.

1. The mixed FE method [Golo et al. 2004], as well as the pseudo-spectral approach [Moulla et al. 2012] lead to finite-dimensional approximate state space models which feature a direct feedthrough between in- and outputs at opposite terminals. This fact can be nicely used to generate inverse models for inversion-based feedforward control [Kotyczka and Blancato 2015]. It is, however, at odds with the finite propagation speed in hyperbolic systems.

2. The direct feedthrough does *not* appear in the mixed FE approach presented in Farle et al. [2013], nor the explicit simplicial discretization of Seslija et al. [2014] where the state/flow variables are defined on dual meshes.

3. The approach of Golo et al. [2004] features a parameter α which contains information on the approximation forms on both energy domains. Using the same forms for both domains, $\alpha = \frac{1}{2}$ is the only value to satisfy the compatibility conditions of the approach. On the other hand, α and $1-\alpha$ appear as factors to compute the co-state variables at each interval from the boundary efforts. Using (disregarding the compatibility conditions) $\alpha = 0$ or $\alpha = 1$, the feedthrough disappears, see e. g. Hamroun et al. [2008]. The state representation then coincides with the one obtained by simplicial discretization or the basic FV method as presented below.

4. PH FINITE VOLUME DISCRETIZATION

In a finite volume numerical approximation which is supposed to preserve the PH structure we replace the flow end effort variables $\boldsymbol{f}^q, \boldsymbol{f}^p, \boldsymbol{e}^q, \boldsymbol{e}^p$ by their *numerical counterparts* $\boldsymbol{F}^q, \boldsymbol{F}^p, \boldsymbol{E}^q, \boldsymbol{E}^p$. At the same time we preserve the boundary input variables $\boldsymbol{E}^b = \boldsymbol{e}^b$ and approximate the collocated outputs $\boldsymbol{F}^b \approx \boldsymbol{f}^b$. In contrast to (34), (35), where the elements of $\boldsymbol{f}^q$, $\boldsymbol{f}^p$ equal the *net fluxes* to each cell, $\boldsymbol{F}^q$, $\boldsymbol{F}^p$ are identified with *net numerical fluxes* computed from the numerical efforts $\boldsymbol{E}^q$, $\boldsymbol{E}^p$. As usual in higher order finite volume methods, the information of multiple adjacent control volumes can be used to approximate the boundary fluxes. The presented finite-dimensional models result from a semi-discrete adaptation of the generalized leapfrog schemes of Iserles [1986] to the open PH setting, putting attention to the definition of boundary in- and outputs.

4.1 Main result

As a main result, we formulate a class of FV semi-discretization schemes which numerically approximate (34), (35) and the power balance (38). For brevity we present only the case of a Hamiltonian independent of the spatial variable z. After some comments on consistency order and convergence, Section 5 illustrates and compares the approach using the (z-dependent) benchmark example from Golo et al. [2004].

The numerical approximate models will have the explicit PH representation

$$\begin{bmatrix} \boldsymbol{F}^q \\ \boldsymbol{F}^p \end{bmatrix} = \begin{bmatrix} \boldsymbol{0} & \bar{\boldsymbol{D}} \\ -\bar{\boldsymbol{D}}^T & \boldsymbol{0} \end{bmatrix} \begin{bmatrix} \boldsymbol{E}^q \\ \boldsymbol{E}^p \end{bmatrix} + \begin{bmatrix} \bar{\boldsymbol{g}}_q & \boldsymbol{0} \\ \boldsymbol{0} & \bar{\boldsymbol{g}}_p \end{bmatrix} \begin{bmatrix} E_L^b \\ E_R^b \end{bmatrix} \tag{39}$$

$$-\begin{bmatrix} F_L^b \\ F_R^p \end{bmatrix} = \begin{bmatrix} \bar{\boldsymbol{g}}_q^T & \boldsymbol{0}^T \\ \boldsymbol{0}^T & \bar{\boldsymbol{g}}_p^T \end{bmatrix} \begin{bmatrix} \boldsymbol{E}^q \\ \boldsymbol{E}^p \end{bmatrix}. \tag{40}$$

The vectors of discrete flow variables

$$\boldsymbol{F}^q = \dot{\boldsymbol{Q}}, \quad \boldsymbol{F}^p = \dot{\boldsymbol{P}} \tag{41}$$

denote the time derivatives of the approximate conserved quantities Q_i, P_i on each cell $\mathcal{C}_i^q$, $\mathcal{C}_i^p$, $i = 1, \dots N$ (discrete state variables), according to Eq. (8). The numerical efforts $\boldsymbol{E}^q$, $\boldsymbol{E}^p$ are derived from the discrete energy approximation

$$\bar{H}(\boldsymbol{Q}, \boldsymbol{P}) = \sum_{i=1}^{N} \mathcal{H}(\frac{Q_i}{\Delta z}, \frac{P_i}{\Delta z})\Delta z \tag{42}$$

according to

$$E_i^q = \frac{\partial}{\partial Q_i}\bar{H}(\boldsymbol{Q},\boldsymbol{P}) = \frac{\partial}{\partial q_i}\mathcal{H}\circ(\frac{Q_i}{\Delta z},\frac{P_i}{\Delta z}) = e_i^q(\frac{Q_i}{\Delta z},\frac{P_i}{\Delta z}), \tag{43}$$

$$E_i^p = \frac{\partial}{\partial P_i}\bar{H}(\boldsymbol{Q},\boldsymbol{P}) = \frac{\partial}{\partial p_i}\mathcal{H}\circ(\frac{Q_i}{\Delta z},\frac{P_i}{\Delta z}) = e_i^p(\frac{Q_i}{\Delta z},\frac{P_i}{\Delta z}). \tag{44}$$

Proposition 2. The PH state representation (39), (40) with matrices

$$\bar{\boldsymbol{D}} = \begin{bmatrix} -a_1 & -a_2 & \cdots & -a_r & & \\ a_1 & -a_1 & \ddots & & \ddots & \\ \vdots & \ddots & \ddots & & & -a_r \\ a_r & & & & \ddots & \vdots \\ & \ddots & & \ddots & \ddots & -a_2 \\ & & a_r & \cdots & a_1 & -a_1 \end{bmatrix}, \ \bar{\boldsymbol{g}}_q = \begin{bmatrix} b_1 \\ \vdots \\ b_r \\ 0 \\ \vdots \\ 0 \end{bmatrix}, \ \bar{\boldsymbol{g}}_p = \begin{bmatrix} 0 \\ \vdots \\ 0 \\ -b_r \\ \vdots \\ -b_1 \end{bmatrix}, \tag{45}$$

energy approximation (42) and constitutive equations (43), (44), is a finite dimensional approximation of a system of two conservation laws in PH form if the coefficients a_i, $i = 1, \dots, r$ are computed from Eq. (12) and

$$b_k = \sum_{i=k}^{r} a_i, \quad k = 1, \dots, r. \tag{46}$$

The consistency order of the approximation inside the spatial domain is $2r$. The approximate power balance

$$(\boldsymbol{E}^q)^T \boldsymbol{F}^q + (\boldsymbol{E}^p)^T \boldsymbol{F}^p + (\boldsymbol{E}^b)^T \boldsymbol{F}^b = 0 \tag{47}$$

converges to (38) for $\Delta z \to 0$.

Proof. The consistency of the numerical approximation is commented in the following subsection. Here, we sketch the convergence of the discretized power balance (47) – which follows from the PH structure of (39), (40) – to (38) for $\Delta z \to 0$.

- The discrete effort variables tend to their continuous versions, see Eqs. (42)–(44): $E_i^q \to e_i^q(z_i^q) = e_i^q$ and $E_i^p \to e_i^p(z_i^p) = e_i^p$ for $i = 1, \dots, N$.
- The same holds for the discrete flows due to the consistency of the method (see below): $F_i^q \to f_i^q$ and $F_i^p \to f_i^p$ for $i = 1, \dots, N$.
- The boundary inputs $\boldsymbol{E}^b = [e^p(z_L)\ e^q(z_R)]$ coincide in the original and discretized case. From the structural identity of (38) and (47) and the convergence of flows and efforts, also $-\boldsymbol{F}^b \to [e^q(z_L)\ -e^p(z_R)]$ follows.

Moreover, it can be verified that the steady state gains from E_L^b to F_R^b and from E_R^b to F_L^b are of magnitude 1 which confirms the conservation of flux.

4.2 Consistency

The consistency order depends on the *local approximation error* made by the use of numerical flux functions. We sketch the consistency analysis for the equations not affected by the boundary inputs, leaving out for the moment the discussion of the boundaries (as a bottleneck for the approximation accuracy of the open system). The net flux to a cell $\mathcal{C}_i^q$, $i = r+1, \dots, N$ on the q grid [6] is

$$f_i^q = e^p(q(z_{i-1}^p), p(z_{i-1}^p)) - e^p(q(z_i^p), p(z_i^p)), \tag{48}$$

whereas the net numerical flux is

$$F_i^q = \sum_{k=1}^{r} a_k E_{i-k}^p(Q_{i-k}, P_{i-k}) - \sum_{k=1}^{r} a_k E_{i-1+k}^p(Q_{i-1+k}, P_{i-1+k}). \tag{49}$$

To determine the local approximation error, the numerical efforts E_j^p are replaced by the expressions (43), (44). Moreover, the discrete state variables Q_j, P_j are replaced by the integrals $\int_{\mathcal{C}_j^q} q(z)dz$, $\int_{\mathcal{C}_j^p} p(z)dz$, assuming the true distribution of the state variables $q(z)$ and $p(z)$. Subtracting (48) from (49) with these replacements, we obtain

$$err_{loc,i}^q = \tag{50}$$
$$\sum_{k=1}^{r} a_k e^p(\frac{\int_{\mathcal{C}_{i-k}^q} q(z)dz}{\Delta z}, \frac{\int_{\mathcal{C}_{i-k}^p} p(z)dz}{\Delta z}) - e^p(q(z_{i-1}^p), p(z_{i-1}^p))$$
$$-\sum_{k=1}^{r} a_k e^p(\frac{\int_{\mathcal{C}_{i-1+k}^q} q(z)dz}{\Delta z}, \frac{\int_{\mathcal{C}_{i-1+k}^p} p(z)dz}{\Delta z}) + e^p(q(z_i^p), p(z_i^p)).$$

If the coefficients a_k are computed from Eq. (12), a Taylor series expansion in Δz shows that the approximation error is of order $\mathcal{O}(\Delta z^{2r+1})$. Hence, the presented family of FV discretization schemes has consistency order $2r$.

4.3 Convergence

The Lax equivalence theorem (see Iserles [2009] for a semi-discrete formulation) allows concluding convergence to the exact solution of a *linear* PDE provided it is well-posed, the numerical scheme is of order ≥ 1 and numerically stable. In the *linear case* (i. e. with quadratic Hamiltonian), well-posedness is a property that can be systematically verified for boundary control systems in PH form [Jacob and Zwart 2012]. The above FV schemes are of order ≥ 2, and for the linear case, exponential growth bounds can be given for the numerical solution $\begin{bmatrix}\boldsymbol{Q}(t)^T & \boldsymbol{P}(t)^T\end{bmatrix}^T$ in any interval $[0, t^*]$. The discussion of convergence in the nonlinear case is more delicate, see e. g. Section 12.12 in LeVeque [2002], and is left for future work.

5. EXAMPLE

As an illustrative example we consider the transmission line of length $L = e - 1$ and non-constant inductance and capacitance per length $l(z) = c(z) = 1/(z+1)$, terminated by a resistance $R = 1$ at $z = L$ as presented in Golo et al. [2004]. The PH PDE is (17) with $q(z,t)$ and $p(z,t) = \psi(z,t)$ the charge and flux density per length, $e^q(z,t) = v(z,t)$ and $e^p(z,t) = i(z,t)$ the voltage and current distributions. For an input voltage $u(t) = e^q(0,t)$, the non-collocated output voltage at the opposite terminal can be computed as $y(t) = e^q(L,t) = u(t - ln(z+1))$.

In Fig. 3, we show (a) the input $u(t)$ and exact output $y(t)$ and (b) three numerical FV solutions $y_{FV,r}(t)$ with $r \in \{1, 2, 4\}$. In the third plot (c) the mixed FE approximation from Golo et al. [2004] is reproduced with parameter

[6] Completely analogous for cell $\mathcal{C}_i^p$, $i = 1, \dots, N - r$ on the p grid.

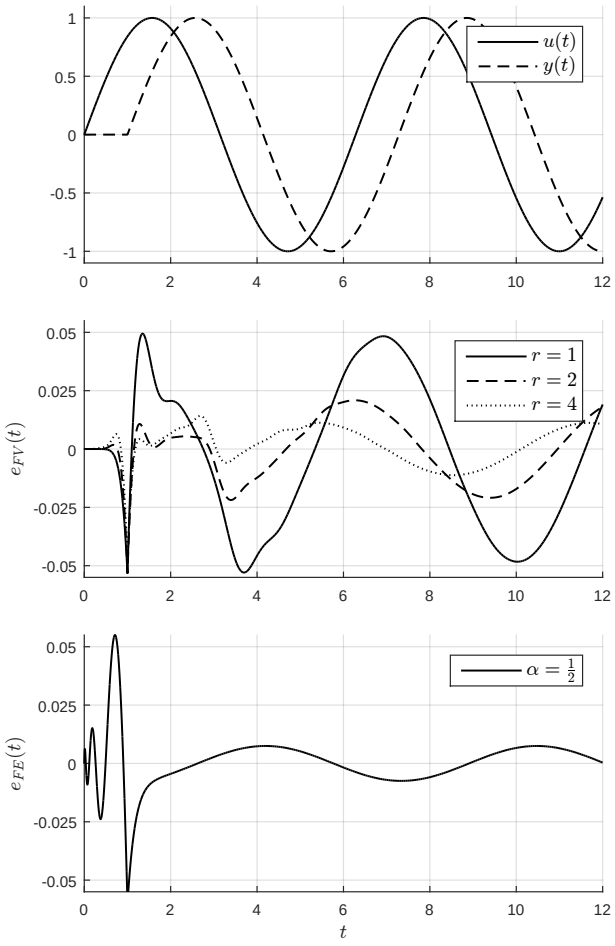

Fig. 3. Simulations of the non-constant transmission line. (a) Input and exact output voltage, (b) FV output error with three different stencils, (c) mixed FE simulation with $\alpha = 1/2$.

$\alpha = \frac{1}{2}$ ("Exp. 4", spline approximation by Whitney forms, uniform grid) for comparison.

Each numerical experiment is based on a discretization with $N = 5$ segments, the lumped inductances, capacitances have been computed according to the expression indicated in Golo et al. [2004] for "Exp. 4", replacing the cell centers on the accordingly shifted grids. The discretized models being linear, the simulations are conducted with MATLAB's *lsim* with a step size of $h = 0.001$.

Avoiding a direct feedthrough in the discretized PH model, the FV scheme with staggered grids approximates the delay of the analytic solution in a non-oscillatory manner in the time interval $t \in [0, 1)$, in contrast to the mixed FE approximation. Increasing the order of the method by a wider stencil, the error $y_{FV,r}(t) - y(t)$ decreases for a fixed number of segments. The magnitude of the initial error around $t = 1$ remains practically unchanged. Increasing the number of segments [7], the error norm of the numerical output decreases, yet not with order $(1/N)^{2r}$. This is due to the fact that no special measures to increase the accuracy at the boundaries, like appropriate *ghost cells*, have been implemented for the simulations.

[7] which is not displayed for space limitation

6. CONCLUSIONS

The proposed family of semi-discrete FV schemes provides ODE (control) models for the considered class of distributed-parameter PH systems with a given accuracy inside the spatial domain. An advantage compared to higher order FE or collocation methods is that the energy approximation to compute the co-state variables remains simple. The "parasitic" feedthrough which is present in some current structure-preserving methods is avoided. To increase the accuracy at the boundaries, additional measures have to be taken. The extension to higher spatial dimensions is conceptually simple in the FV perspective and is a topic of ongoing work, as well as the full-discretization to obtain multi-symplectic schemes for PH systems.

REFERENCES

Eymard, R., Gallouët, T., and Herbin, R. (2000). Finite volume methods. *Handbook of numerical analysis*, 7, 713–1018.

Farle, O., Klis, D., Jochum, M., Floch, O., and Dyczij-Edlinger, R. (2013). A port-Hamiltonian finite-element formulation for the Maxwell equations. In *Proc. IEEE Int. Conf. on Electromagnetics in Advanced Applications (ICEAA), Torino, Italy*, 324–327.

Fornberg, B. and Ghrist, M. (1999). Spatial finite difference approximations for wave-type equations. *SIAM Journal on Numerical Analysis*, 37(1), 105–130.

Golo, G., Talasila, V., van der Schaft, A., and Maschke, B. (2004). Hamiltonian discretization of boundary control systems. *Automatica*, 40(5), 757–771.

Hamroun, B., Lefèvre, L., and Mendes, E. (2008). Passivity based control of a reduced port-controlled Hamiltonian model for the shallow water equations. In *Proc. 47th IEEE Conf. Decision and Control, Cancun, Mexico*, 3917–3922.

Iserles, A. (1986). Generalized leapfrog methods. *IMA Journal of Numerical Analysis*, 6(4), 381–392.

Iserles, A. (2009). *A first course in the numerical analysis of differential equations*. Cambridge University Press.

Jacob, B. and Zwart, H. (2012). *Linear port-Hamiltonian systems on infinite-dimensional spaces*, volume 223. Springer.

Kotyczka, P. and Blancato, A. (2015). Feedforward control of a channel flow based on a discretized port-Hamiltonian model. *IFAC-PapersOnLine*, 48(13), 194–199. 5th IFAC Workshop on Lagrangian and Hamiltonian Methods for Nonlinear Control, Lyon, France.

LeVeque, R.J. (1992). *Numerical methods for conservation laws*, volume 132 of *Lectures in Mathematics: ETH Zürich*. Springer.

LeVeque, R.J. (2002). *Finite volume methods for hyperbolic problems*, volume 31. Cambridge University Press.

Moulla, R., Lefévre, L., and Maschke, B. (2012). Pseudo-spectral methods for the spatial symplectic reduction of open systems of conservation laws. *Journal of Computational Physics*, 231(4), 1272–1292.

Ramirez, H., Gorrec, Y.L., Macchelli, A., and Zwart, H. (2014). Exponential stabilization of boundary controlled port-Hamiltonian systems with dynamic feedback. *IEEE Transactions on Automatic Control*, 59(10), 2849–2855.

Rezzolla, L. (2011). *Numerical Methods for the Solution of Partial Differential Equations*. Lecture Notes, available online (www.aei.mpg.de/~rezzolla).

Seslija, M., Scherpen, J.M.A., and van der Schaft, A.J. (2014). Explicit simplicial discretization of distributed-parameter port-Hamiltonian systems. *Automatica*, 50(2), 369–377.

van der Schaft, A.J. and Maschke, B.M. (2002). Hamiltonian formulation of distributed-parameter systems with boundary energy flow. *Journal of Geometry and Physics*, 42(1), 166–194.

Yee, K.S. et al. (1966). Numerical solution of initial boundary value problems involving Maxwells equations in isotropic media. *IEEE Trans. Antennas Propag*, 14(3), 302–307.